Thermomechanical properties and thermal degradation kinetics of poly(methyl methacrylate) (PMMA) and polycarbonate (PC) filled with cerium-doped yttrium aluminium garnet (Ce:YAG) prepared by melt compounding

M. A. Sibeko, A. S. Luyt & M. L. Saladino

Polymer Bulletin

ISSN 0170-0839
Volume 74
Number 7

Polym. Bull. (2017) 74:2841-2859
DOI 10.1007/s00289-016-1870-5

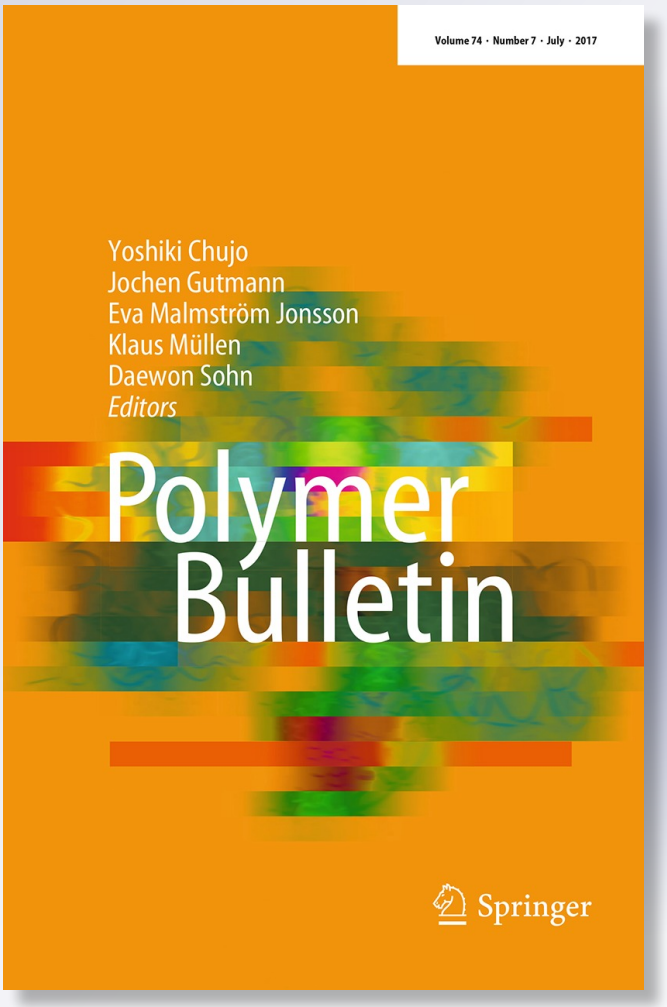

Springer

Polym. Bull. (2017) 74:2841–2859
DOI 10.1007/s00289-016-1870-5

ORIGINAL PAPER

Thermomechanical properties and thermal degradation kinetics of poly(methyl methacrylate) (PMMA) and polycarbonate (PC) filled with cerium-doped yttrium aluminium garnet (Ce:YAG) prepared by melt compounding

M. A. Sibeko[1] · A. S. Luyt[2] · M. L. Saladino[3,4]

Received: 23 May 2016 / Revised: 10 November 2016 / Accepted: 26 November 2016 /
Published online: 2 December 2016

Abstract This paper reports on the thermomechanical properties and thermal degradation kinetics of poly(methyl methacrylate) (PMMA) and polycarbonate (PC) composites filled with cerium-doped yttrium aluminium garnet (Ce:YAG) at different contents ranging between 0.1 and 5 wt%, and prepared by melt compounding. The interaction between PMMA and the filler was much stronger than that between PC and the filler, and this resulted in a significant improvement in the dynamic mechanical properties of the PMMA composites. The presence of filler did not significantly increase the thermal stability of the PC, while an observable increase in the thermal stability was only observed at higher filler loadings for the PMMA composites. This was attributed to the stronger interaction between Ce:YAG and PMMA and/or its degradation volatiles.

Keywords Poly(methyl methacrylate) · Polycarbonate · Yttrium aluminium garnet doped with cerium · Thermomechanical properties · Thermal degradation kinetics

✉ A. S. Luyt
aluyt@qu.edu.qa

[1] Department of Chemistry, University of the Free State (Qwaqwa Campus), Private Bag X13, Phuthaditjhaba 9866, South Africa

[2] Center for Advanced Materials, Qatar University, PO Box 2713, Doha, Qatar

[3] Dipartimento Scienze e Tecnologie Biologiche, Chimiche e Farmaceutiche-STEBICEF and INSTM UdR-Palermo, Università di Palermo, Parco d' Orleans II, Viale delle Scienze pad.17, 90128 Palermo, Italy

[4] Centro Grandi Apparecchiature-AteN center, Università di Palermo, Via F.Marini 14, 90128 Palermo, Italy

Introduction

For a number of decades, inorganic nanofillers, which include nanoclays, carbon nanotubes, graphite, silver, carbon black, titania, nanowhiskers and mesoporous silica, had been used to improve the properties of polymers. The novel properties that result from the mutual interaction between the polymer and the filler are beneficial not only for basic research purpose but also for the development of industrial applications [1–4]. The incorporation of phosphorescent nanoparticles (PNP) into polymers to improve their limitational applications has recently been studied. Phosphorescent nanoparticles are solid materials that emit light, or luminesce, when exposed to radiation such as ultraviolet light or an electron beam. They are of special interest today due to their broad range of applications, from solid-state lighting and novel flat displays to high-resolution X-ray detectors and sensors in biomedicine [5–8].

The yttrium–alumina (Y_2O_3–AI_2O_3) system has three compounds that are stable at room temperature and are classified according to their molar ratio and thermodynamic condition. These are yttrium aluminium garnet (YAG), yttrium aluminium perovskite (YAP), and the symmetric yttrium aluminium monoclinic structures (YAM). YAG has received the most attention because of its interesting optical and mechanical properties, and high-temperature creep resistance. The pure YAG phase is favourable for the luminescent properties of phosphors, but it needs to be synthesized by a solid-state reaction at a high temperature near 1600 °C to obtain it in a pure state without the intermediate phases (YAM, YAP). As a result, the powders are non-homogeneous, large in size and have irregular shapes, which negatively affect the luminescent properties. A number of soft chemical preparation methods have been developed to reduce the synthesis temperature and to obtain phosphorescent nanoparticles with controlled particle size [9–14]. These methods include hydrothermal [15], glycothermal [16], sol–gel [17] and spray–pyrolysis synthesis [18], as well as combustion [19], co-precipitation of hydroxides [7, 20], microwave-assisted synthesis [21], and synthesis in a confined environment [22]. All these methods are promising because the morphology and particle size can be controlled. YAG is a good host material for rare-earth-based phosphors and is widely used in optical and electronics applications due to its good thermal stability, and excellent optical and mechanical properties [23].

Polymer phosphorescent nanoparticle composites have recently been considered as potential candidates for the development of light-emitting diodes (LEDs). Polymers such as poly(methyl methacrylate) (PMMA) and polycarbonate (PC) are adequate matrices due to their good light transmittance, their excellent mechanical properties, and their low cost [24–27]. A few authors studied the effect of phosphorescent nanoparticles on the thermal properties of PMMA prepared by a solution-mixing method [24–28], and it was found that the thermal stability of PMMA generally increased with an increase in the nano-phosphorescent content. Zanotto et al. [28] studied the effect of Ce:YAG and CoHCF on the thermal stability of PMMA at 5 wt% Ce:YAG loading. They observed an insignificant increase in the thermal stability of PMMA in the presence of CoHCF and an almost 50 °C

improvement in the presence of Ce:YAG. This was attributed to the better dispersed Ce:YAG nanoparticles, and to a strong interaction with PMMA, which not only immobilized the polymer chains but also the free radicals that take part in the degradation process. The degradation of PMMA and PC composites has also been studied by a number of research groups using the Flynn–Wall–Ozawa [29–31] and Kissinger–Akahira–Sunose methods [30, 32]. These studies showed that the degradation temperature and activation energy of PMMA and PC increased with the addition of nanoparticles. This was attributed to the large surface area of the nanoparticles and the fact that the particles might have trapped radicals during degradation, making the polymer more thermally stable because more energy was required to initiate the degradation process. However, some studies observed a decrease in the activation energy at low filler loadings, and this was attributed to the catalytic effect of the nanoparticles.

There are number of papers that reported on the thermomechanical properties of PMMA and PC nanocomposites [33–37]. Generally, the addition of filler increased the storage modulus and loss modulus, and this was mostly attributed to the reinforcing effect of the nanofillers because of their high aspect ratios and interaction with the polymer chains. Apparently, the formation of crystalline domains around the nanoparticles effectively improved the interaction between the particles and the polymer chains. Musbah et al. [38, 39] introduced Y_2O_3:Eu^{3+} and Eu:Gd_2O_3 into PMMA using a laboratory mixing moulder. The presence of filler increased the storage modulus, loss modulus and glass transition temperature of PMMA. To the best of our knowledge, there are no reports on the thermomechanical properties of PC phosphorescent composites.

The morphology, structure and the luminescence properties of the PMMA/Ce:YAG and the PC/Ce:YAG composites, investigated in this article, were studied using different techniques [40, 41]. The TEM micrographs of the PMMA/Ce:YAG composites with 0.5 wt% loading showed isolated Ce:YAG clusters due to the small amount of filler, which was also not detected in the XRD analysis, but at higher filler loadings, smaller and better dispersed Ce:YAG clusters were observed, which was attributed to the higher viscosity of the sample during mixing. The TEM micrographs of the PC/Ce:YAG composites loaded with 0.5 wt% also showed isolated Ce:YAG particles, while the samples with higher loadings showed larger particles. NMR investigation showed that the interaction between the two polymers and the Ce:YAG particles was an electron donor–acceptor interaction between the carbonyl oxygen lone pair of the polymers and the yttrium ion (Y^{3+}). However, PMMA showed stronger interaction than PC, which was attributed to the carbonyl oxygen on PMMA having a stronger partially negative charge. The Commission Internationale de l'Eclairage (CIE) (x, y) coordinates of the light obtained when combining blue LEDs with the PMMA/Ce:YAG composite with 5 wt% Ce:YAG and the PC/Ce:YAG composite with 2 wt% Ce:YAG were located in the white region, making these composites suitable for applications in white-light-emitting diodes.

In this article, the effect of Ce:YAG on the thermomechanical properties, as well as the thermal degradation kinetics, of PMMA and PC has been studied by means of dynamic mechanical analysis (DMA) and thermogravimetric analysis (TGA).

Materials and methods

Materials

Commercial-grade PMMA (Altuglas® V920T), having a melt flow rate of 1 g/10 min at 230 °C/3.8 kg and $M_w = 110{,}000$ g mol^{-1}, produced by Bayer Materials Science, Italy, was obtained in pellet form. Commercial-grade bisphenol-A polycarbonate (Makrolon® 2407), with a melt flow rate of 20 g/10 min at 300 °C/1.2 kg and $M_w = 57{,}404$ g mol^{-1}, was obtained in pellet form from Bayer Material Science, Germany. Yttrium aluminium garnet doped with cerium (Ce:YAG), with a density of 4.8 g cm^{-3}, was supplied as a yellow powder by Dongtai Tianyuan Fluorescent Materials, China and was used as received.

Preparation of the PMMA/Ce:YAG and PC/Ce:YAG composites

The PMMA and PC pellets, and Ce:YAG powder, were dried in an oven at 80 °C for 12 h before preparation. All the composites were prepared using a Brabender Plastograph 50 mL melt-mixer at 200 °C and 50 rpm for 10 min. For the preparation of the composites, the polymers were first melted for 2 min at 200 °C without nitrogen flush, and different contents (0.1, 0.3, 0.5, 1, 2 and 5 wt%) of the Ce:YAG were added into the molten polymer and mixed for a further 8 min. The samples were then melt-pressed (in the absence of vacuum) into 3-mm-thick sheets at 200 °C for 5 min at 50 bar. The neat polymers as control samples were prepared following the same procedure.

Sample analysis

Dynamic mechanical analysis (DMA) was performed from 40 to 180 °C for all the samples under nitrogen flow in a bending (dual cantilever) mode at a heating rate of 5 °C min^{-1} and a frequency of 1 Hz using a PerkinElmer Diamond DMA from Waltham, Massachusetts, USA.

A PerkinElmer STA 6000 thermogravimetric analyser (TGA) was used to analyse the thermal degradation behaviour of the samples. The analyses were done from 30 to 700 °C at a heating rate of 10 °C min^{-1} under nitrogen flow (20 ml min^{-1}). The sample masses ranged between 20 and 25 mg. The samples for thermal degradation kinetics were run at 3, 5, 7 and 9 °C min^{-1} heating rates under nitrogen flow (20 ml min^{-1}), and the TGA's integrated kinetics software [based on the Flynn–Ozawa–Wall method (Eq. 1)] was used to calculate the activation energies.

$$\ln \beta = c - 1.052\left(\frac{E_a}{\mathrm{RT}}\right) \tag{1}$$

where β is the heating rate in K min^{-1}, c is a constant, E_α is the activation energy in kJ mol^{-1}, R is the universal gas constant, and T is the temperature in K. The plot of

ln β vs. $1/T$, obtained from the TGA curves recorded at several heating rates, should be a straight line. The activation energy was evaluated from its slope.

Results and discussion

Dynamic mechanical analysis (DMA)

The storage modulus curves of PMMA and the PMMA/Ce:YAG composites are reported in Fig. 1, and the E' values taken at 70 and 140 °C are reported in Table 1, and Fig. 2 shows the storage modulus curves of PC and the PC/Ce:YAG composites as a function of temperature, and the E' values taken at 100 and 170 °C are also reported in Table 1. Below the glass transition temperature, the storage modulus of both polymers increases with the addition of Ce:YAG. However, the amount of Ce:YAG particles had little influence on the values of E', and there is no clear trend in the effect of filler on the storage modulus at these temperatures (Table 1). This is probably because the hard, brittle polymers and the Ce:YAG particles have very similar stiffness values in this temperature range. The higher storage modulus values above the glass transition temperature for the two polymers can be attributed to the immobilization of the polymer chains through interaction with the filler particles, and the increase in the rigidity of the composite as a result of the inherent stiffness of the filler. The interaction was confirmed to be an electron donor–acceptor interaction between the carbonyl oxygen lone pair on the polymers and the yttrium cation (Y^{3+}) in Ce:YAG [40, 41]. However, there was no clear trend in the effect of the filler on the E' values of the two polymers (Table 1). Musbah et al. [39] observed a similar increase in the storage modulus of PMMA after the addition of europium-doped gadolinium oxide (Eu:Gd_2O_3). They attributed it to a reduction in the overall mobility of the polymer chains because of functional physical crosslinks between the polymer and filler.

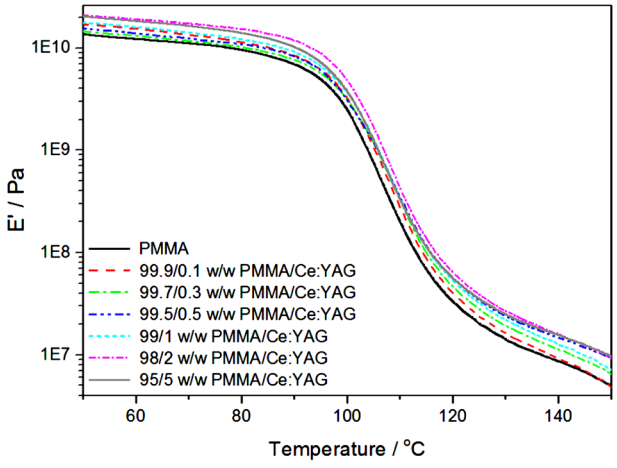

Fig. 1 Storage modulus curves of PMMA and the PMMA/Ce:YAG composites

Table 1 DMA results of PMMA, PC, and their respective composites with Ce:YAG

Sample	PMMA			
	10^{-10} E'/Pa at 70 °C	10^{-7} E'/Pa at 140 °C	T_g/°C from E'' curves	T_g/°C from tan δ curves
PMMA	1.3	0.8	95.3	114.7
99.9/0.1 w/w PMMA/Ce:YAG	1.4	0.9	96.7	114.8
99.7/0.3 w/w PMMA/Ce:YAG	1.2	1.1	96.3	114.5
99.5/0.5 w/w PMMA/Ce:YAG	1.2	1.5	96.5	114.5
99/1 w/w PMMA/Ce:YAG	1.4	1.2	97.5	114.1
98/2 w/w PMMA/Ce:YAG	1.7	1.6	98.1	114.1
95/5 w/w PMMA/Ce:YAG	1.6	1.5	97.7	113.9
Sample	PC			
	10^{-10} E'/Pa at 100 °C	10^{-8} E'/Pa at 170 °C	T_g/°C from E'' curves	T_g/°C from tan δ curves
PC	1.6 ± 0.1	0.9 ± 0.0	147.1	154.1
99.9/0.1 w/w PC/Ce:YAG	2.2 ± 0.0	2.8 ± 0.1	146.9	154.1
99.7/0.3 w/w PC/Ce:YAG	1.8 ± 0.0	1.9 ± 0.3	147.2	154.5
99.5/0.5 w/w PC/Ce:YAG	2.0 ± 0.1	0.8 ± 0.0	147.0	154.6
98/2 w/w PC/Ce:YAG	1.7 ± 0.3	2.7 ± 0.2	147.4	154.7
95/5 w/w PC/Ce:YAG	1.7 ± 0.0	1.6 ± 0.0	146.1	154.1

The maximum increase in storage modulus of PC above the glass transition temperature was observed at 0.1 wt% Ce:YAG loading, which is probably due to the reinforcing effect of the good dispersion and small sizes of the Ce:YAG particles, which we observed from TEM micrographs [41]. The storage modulus of the samples containing 0.3 and 0.5 wt% Ce:YAG was lower, and at 0.5 wt% Ce:YAG, the storage modulus was almost the same as that of pure PC. At the highest filler loadings (2 and 5 wt%), there was no clear trend on the influence of the filler on the E' values. This behaviour can be attributed to the weak interaction between the polymer and the filler as a result of the presence of filler agglomerates. Suin et al. [42] observed a definite increase in storage modulus of PC throughout the investigated temperature range with an increase in clay loading. They attributed this to the reinforcing effect imparted by the high aspect ratio of the clay platelets, which caused a greater degree of stress transfer at the interface. However, Motaung et al. observed a decrease in storage modulus of PC with the addition of titania [43] and zirconia [44] nanoparticles at 1 and 2 wt% loadings, which they attributed to a plasticizing effect of the nanoparticles on the polymer matrix.

The loss modulus and tan δ curves of PMMA and the PMMA/Ce:YAG composites as function of temperature are shown in Figs. 3 and 4, and the glass transition temperatures taken from the E'' and tan δ curves are summarised in Table 1. The loss modulus also increased for the filler-containing samples, as was observed and discussed for the storage modulus. The addition of filler resulted in an observable increase in the glass transition temperature from the loss modulus curves

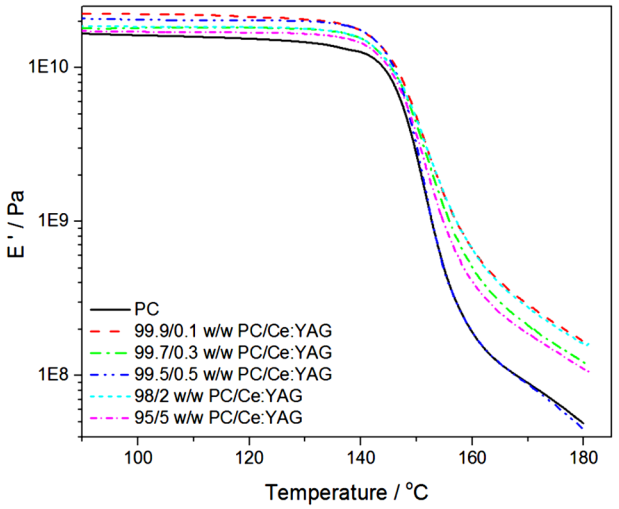

Fig. 2 Storage modulus curves of PC and the PC/Ce:YAG composites

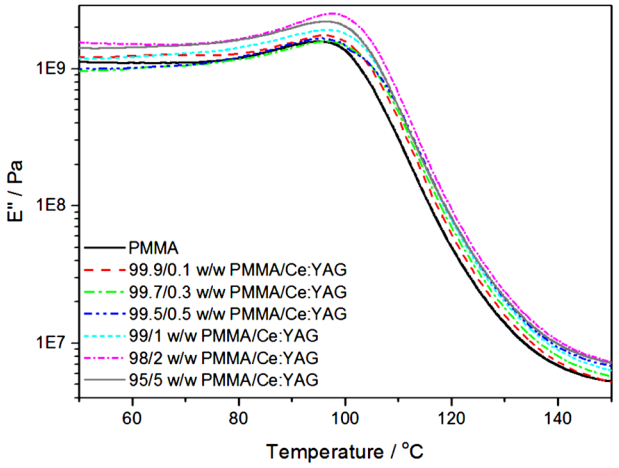

Fig. 3 Loss modulus curves of PMMA and the PMMA/Ce:YAG composites

(Table 1), which can be due to the immobilization of polymer chains which we observed from our NMR investigation [40]. It has been mentioned that, in particulate-filled polymers, the presence of rigid fillers restricts the movement of the polymer chains, leading to a reduction in the maximum value of tan δ and a shift of the T_g values to higher temperatures [45]. This behaviour has been observed for PMMA with the addition of silica [46], organoclay [47], and mesoporous silica particles (MCM-41) [48], and has been attributed to good adhesion between the filler and the matrix, which resulted in a restriction of the mobility of the polymer chains in the composite. However, in our case, the tan δ curves (Fig. 4) do not show

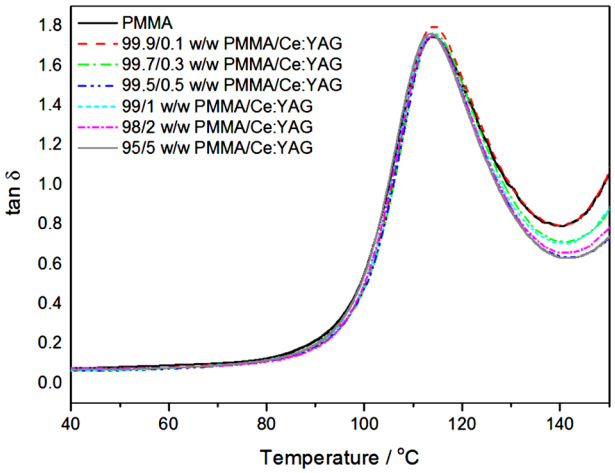

Fig. 4 Tan δ curves of PMMA and the PMMA/Ce:YAG composites

any significant effect of the Ce:YAG particles on the temperature and intensity of the glass transition of PMMA. This is probably because the polymer–filler interaction [40] was not strong enough to significantly immobilize the polymer chains.

The loss modulus and tan δ curves of PC and the PC/Ce:YAG composites are shown in Figs. 5 and 6, and the glass transition temperature values taken from the E″ and tan δ curves are summarised in Table 1. The loss modulus curves show the same inconsistencies as was observed and discussed for the storage modulus. The addition of Ce:YAG had no influence on the glass transition temperature of PC (Table 1), which indicates that the filler had little effect on the polymer chain mobility, which we observed from the NMR results presented and discussed in another paper [41]. Figure 6 shows a significant reduction in the damping after the addition of certain amounts of Ce:YAG, but there was no correlation between the amount of damping and the amount of Ce:YAG mixed into PC. The absence of a change in the glass transition temperature, and the inconsistent change in the amount of damping, confirm that the dynamic mechanical behaviour of the PC/Ce:YAG composites was influenced by a complex set of factors, and that the interaction between PC and Ce:YAG was fairly weak, because a strong interaction would have dominated all the other possible contributing factors and given rise to consistently higher storage moduli and glass transition temperatures, and consistently lower damping.

Thermogravimetric analysis

The TGA curves of PMMA and the PMMA/Ce:YAG composites are shown in Fig. 7, and some of the temperatures are summarised in Table 2. All the samples show one degradation step starting around 330 °C. The thermal stability of PMMA is not significantly influenced by the presence of Ce:YAG up to 2 wt% Ce:YAG,

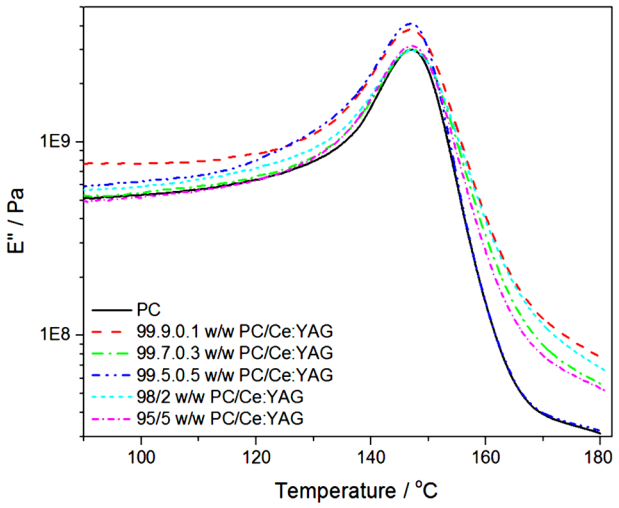

Fig. 5 Loss modulus curves of PC and the PC/Ce:YAG composites

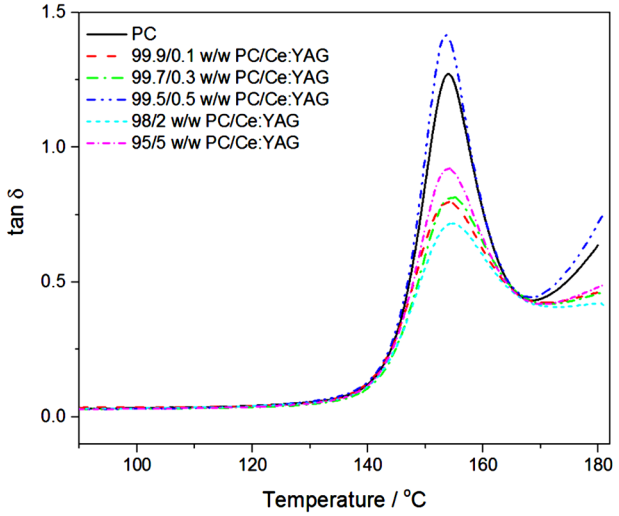

Fig. 6 Tan δ curves of PC and the PC/Ce:YAG composites

and an observable increase was only observed for the sample containing 5 wt% Ce:YAG. The increase in mass loss temperature can be due to some immobilization of the polymer chains, as was observed from our previously presented NMR results [40], and of the free radicals that took part in the degradation process, or to interaction of the volatile degradation products, that are formed during degradation, with the filler particles that caused them to be released at higher temperatures. Another possible reason for the increases in thermal stability of the composites is the difference in the thermal conductivity values of PMMA (0.19 W m^{-1} K^{-1}) [49] and Ce:YAG (11.2 W m^{-1} K^{-1}). The shift in decomposition temperature can be

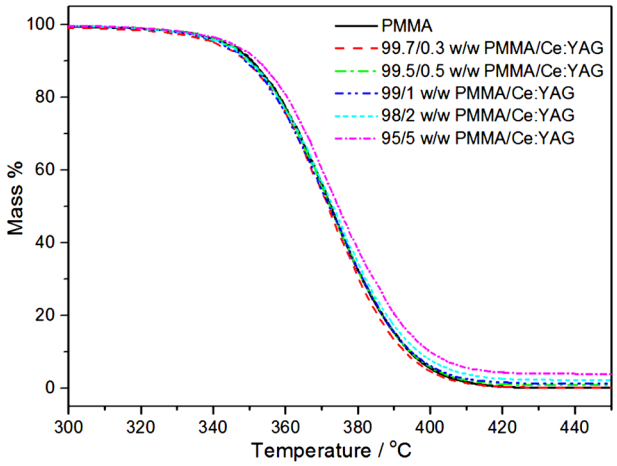

Fig. 7 TGA curves of PMMA and the PMMA/CeYAG composites

Table 2 TGA results for all the investigated samples

Sample	PMMA		
	T_{40}/°C	T_{max}/°C	% Residue at 450 °C
PMMA	368.5	372.7	–
99.7/0.3 w/w PMMA/Ce:YAG	367.4	371.8	0.1
99.5/0.5 w/w PMMA/Ce:YAG	368.2	372.6	0.8
99/1 w/w PMMA/Ce:YAG	367.6	372.0	1.2
98/2 w/w PMMA/Ce:YAG	368.7	373.0	2.1
95/5 w/w PMMA/Ce:YAG	369.9	374.7	4.9
Sample	PC		
	T_{30}/°C	T_{max}/°C	% Residue at 650 °C
PC	491.6	496.3	21.2
99.9/0.1 w/w PC/Ce:YAG	486.2	494.4	21.4
99.7/0.3 w/w PC/Ce:YAG	491.2	501.8	21.6
99.5/0.5 w/w PC/Ce:YAG	492.1	502.4	21.9
99/1 w/w PC/Ce:YAG	488.3	495.7	22.4
98/2 w/w PC/Ce:YAG	489.8	501.6	23.7
95/5 w/w PC/Ce:YAG	488.4	496.2	26.5

T_{30} and T_{40} are the temperatures at 30 and 40% weight loss, while T_{max} is the peak temperature from the derivative TGA curves

attributed to relatively higher thermal conductivity value of Ce:YAG, which caused it to preferentially absorb most of the heat. In this case, the filler acted as a heat barrier and increased the thermal stability of the composites.

Since the mass loss temperature depends on the amount of filler and their dispersion in the composites, and on the interaction of the filler with the polymer chains, free radical chains, and volatile decomposition products, one would expect an increase in mass loss temperature with increasing filler content. In our case, the addition of small amounts of filler resulted in the formation of isolated Ce:YAG clusters (observed in our previously reported TEM micrographs [40]), and thus, less filler surface was exposed to the polymer so that the filler had little influence on the thermal stability of PMMA. However, at higher loadings, smaller Ce:YAG clusters were fairly well dispersed in the polymer and more filler surface was exposed to the polymer. This allowed more effective interaction with the filler so that the polymer and free radical chains were immobilized and/or the volatile degradation products were trapped through their interaction with the filler particles.

The preparation method of the composites can also have a significant influence on the dispersion of the filler in the polymer matrix, and on the influence of the filler on the thermal stability of the composites. Zanotto et al. [28] prepared the same composites by solution mixing and they observed an almost 50 °C improvement in the thermal stability at 5 wt% Ce:YAG loading. They attributed this to the small and well-dispersed Ce:YAG nanoparticles and their strong interaction with the polymer, which not only immobilized the polymer chains but also the free radicals that took part in the degradation process. Although it is difficult to commercialize such a preparation technique, it definitely gave rise to a nanocomposite with very few clusters, which does not seem to be achievable through melt-mixing.

The amounts of residue observed at 450 °C are summarised in Table 2. Generally, the amount of residue corresponds well with the amount of Ce:YAG initially added during the preparation of the composites, suggesting that the dispersion of the Ce:YAG clusters was fairly homogenous in the composites.

Figure 8 shows the TGA curves of PC and the PC/Ce:YAG composites at different Ce:YAG loadings, and some of the temperatures are summarised in Table 2. PC shows no mass loss up to 420 °C, and its decomposition occurs in a single step between 420 and 530 °C. It leaves about 21% residue at 650 °C, and this has also been observed in a number of studies both in air and nitrogen atmospheres [50, 51]. TGA measures mass loss as a function of time or temperature, and any interaction between the volatile degradation products and the filler particles would delay the volatilization of the degradation products, which would increase the temperature at which mass loss occurs. Normally, at high temperatures, the long-chain backbone of a polymer undergoes molecular scission and forms free radicals, which react with each other and with other polymer chains and release volatile products causing a mass loss of the polymer [52]. In our case, the free radicals and volatile degradation products did not seem to interact very strongly with the Ce:YAG particles, because little difference was observed between the TGA curves of the different samples. Other authors reported both an increase [53] and a decrease [54] in the thermal stability of PC in the presence of nanoparticles. The decrease in

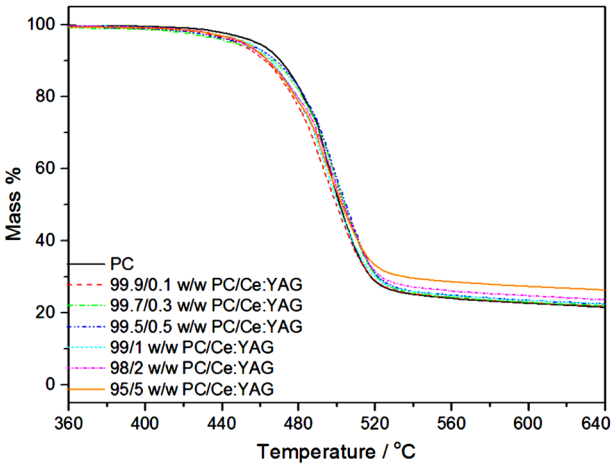

Fig. 8 TGA curves of PC and the PC/Ce:YAG composites

thermal stability was related to the catalytic effect of the nanoparticles, the particle dispersion in the polymer matrix, and the preparation conditions.

The amounts of residue observed at 650 °C for PC and all the composites are summarised in Table 2. The PC/Ce:YAG composites generally left more residue than the neat PC. The differences between the % residues left by the composites, and that left by neat PC, correspond well with the amounts of Ce:YAG initially mixed into the samples, indicating that the dispersion of the Ce:YAG particles was fairly homogenous in the composites.

Thermal degradation kinetics

To get a better understanding of the degradation process and the effect of the Ce:YAG on the thermal stability of PMMA and PC, the activation energy (E_a) for mass loss was determined for the degradation of PMMA, PC and their composites filled with 0.5 and 5 wt% Ce:YAG. The activation energy was determined from the slopes of the isoconversional plots of ln β versus $1/T$ shown in Figs. 9, 10, 11 and 12 taken at heating rates of 3, 5, 7 and 9 °C min^{-1}. The relationship between the activation energies and the extent of mass loss of PMMA/Ce:YAG and the PC/Ce:YAG composites is shown in Figs. 13 and 14. The activation energy is the amount of energy that is required to initiate the thermal degradation process, and it is related to the temperature dependence of the rate of degradation. The activation energy increased with an increase in extent of mass loss for all the investigated samples. The same behaviour was also observed by other authors [55, 56], and it is generally explained as changes in the degradation mechanism with an increase in the extent of mass loss. Dong et al. [31] investigated PC–MgO nanocomposites and they attributed the increase in the activation energy of degradation with an increase in the extent of mass loss to the formation of a stable char which protects the polymer from further degradation.

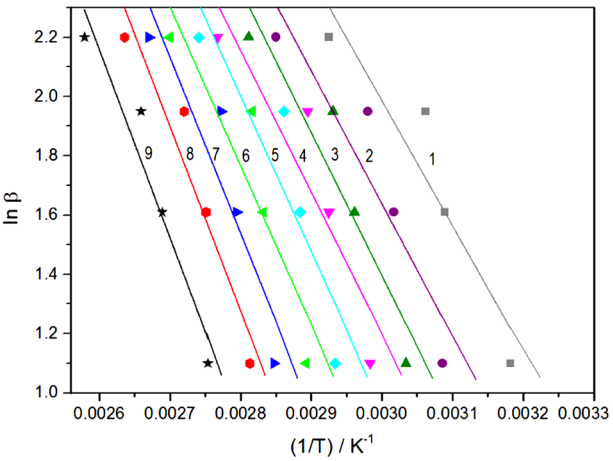

Fig. 9 Ozawa–Flynn–Wall plots derived from the PMMA mass loss curves for the following degrees of conversion: *1* $\alpha = 0.1$; *2* $\alpha = 0.2$; *3* $\alpha = 0.3$; *4* $\alpha = 0.4$; *5* $\alpha = 0.5$; *6* $\alpha = 0.6$; *7* $\alpha = 0.7$; *8* $\alpha = 0.8$; *9* $\alpha = 0.9$

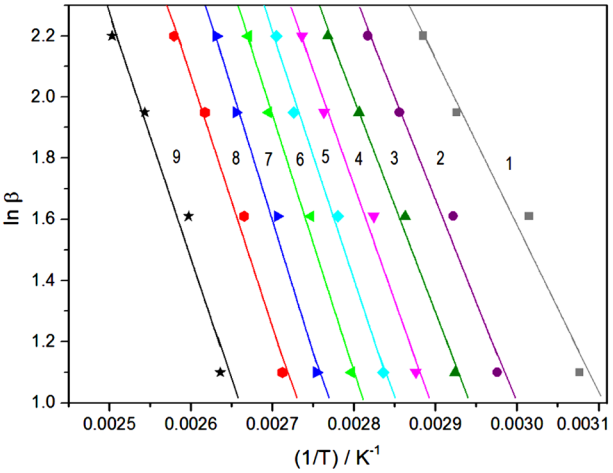

Fig. 10 Ozawa–Flynn–Wall plots derived from the 99.5/5 w/w PMMA/Ce:YAG mass loss curves for the following degrees of conversion: *1* $\alpha = 0.1$; *2* $\alpha = 0.2$; *3* $\alpha = 0.3$; *4* $\alpha = 0.4$; *5* $\alpha = 0.5$; *6* $\alpha = 0.6$; *7* $\alpha = 0.7$; *8* $\alpha = 0.8$; *9* $\alpha = 0.9$

The activation energy of PMMA and its composites shows a general increase with the increase in the extent of mass loss, but the composites show much higher activation energies than the neat polymer. This can be attributed to the trapping of the free radical chains and volatile degradation products by the filler during the degradation process, so that more energy was required to initiate and propagate the degradation of the polymer, or to release the volatile degradation products adsorbed onto the filler particles. The PC composites have much lower activation energy values than the neat PC. This indicates that less energy was required to initiate the

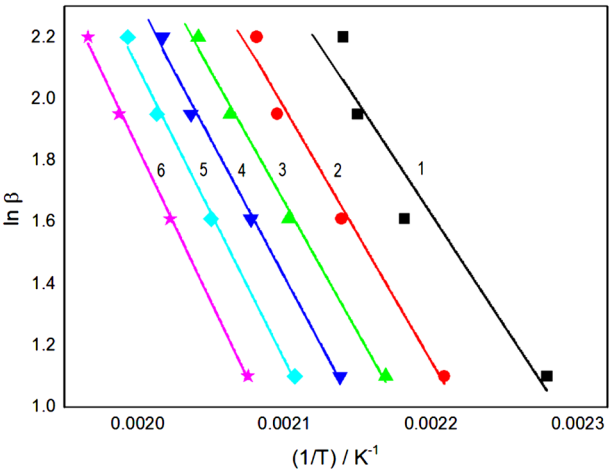

Fig. 11 Ozawa–Flynn–Wall plots derived from the PC mass loss curves for the following degrees of conversion: *1* $\alpha = 0.1$; *2* $\alpha = 0.2$; *3* $\alpha = 0.3$; *4* $\alpha = 0.4$; *5* $\alpha = 0.5$; *6* $\alpha = 0.6$

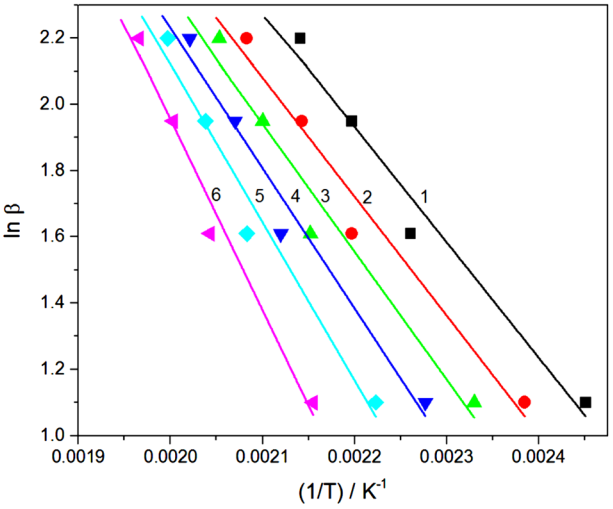

Fig. 12 Ozawa–Flynn–Wall plots derived from the 95/5 w/w PC/Ce:YAG mass loss curves for the following degrees of conversion: *1* $\alpha = 0.1$; *2* $\alpha = 0.2$; *3* $\alpha = 0.3$; *4* $\alpha = 0.4$; *5* $\alpha = 0.5$; *6* $\alpha = 0.6$

degradation process, and that the degradation rates of the composites were less dependent on temperature. Dong et al. [31] observed that the initial activation energy values of the PC–MgO nanocomposites were lower than those of the neat PC. They attributed these observations to the catalytic effect the MgO nanoparticles have on the degradation process of PC. The addition of Ce:YAG in our case may have had a similar catalytic effect on the degradation of PC. An increase in the activation energy values of similar composites was observed in a number of studies [57–59], and these were attributed to the particles acting as physical barriers, both to

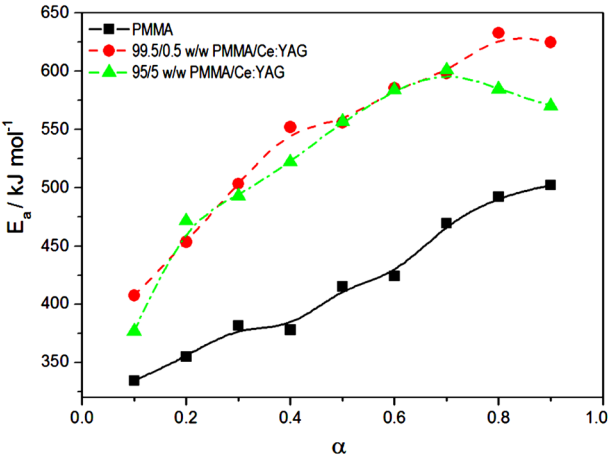

Fig. 13 Activation energy vs. extent of degradation for PMMA and the PMMA/Ce:YAG composites with 0.5 and 5 wt% Ce:YAG

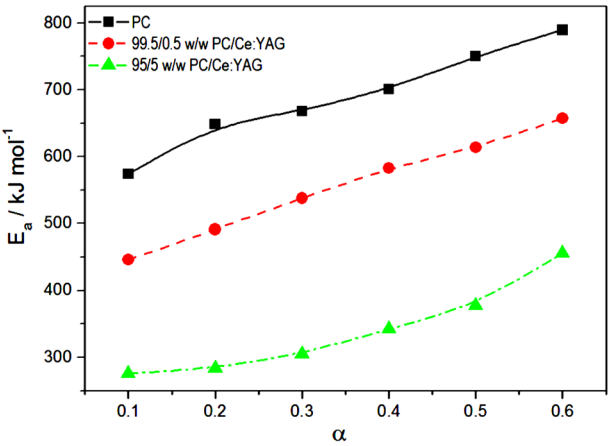

Fig. 14 Activation energy vs. extent of degradation for PC and the PC/Ce:YAG composites with 0.5 and 5 wt% Ce:YAG

retard the thermal decomposition of the polymer and to prevent the transport of volatile degradation products out of the composites, both of which would require more energy to initiate the thermal degradation process.

Conclusions

The purpose of the work reported in this article was to investigate the influence of the presence of different amounts of cerium-doped yttrium aluminium garnet (Ce:YAG) ranging from 0.1 to 5 wt% on the thermomechanical properties and

thermal degradation kinetics of PMMA and PC composites. The presence of filler did not significantly increase the thermal stability of the PC, while an observable increase in thermal stability was only observed at higher filler loadings for the PMMA composites. This can be due to the stronger interaction between Ce:YAG and PMMA and/or its degradation volatiles. The degradation products of PC are carbon dioxide, phenol and bisphenol A, most of which should not strongly interact with Ce:YAG, while that of PMMA is methyl methacrylate, which should interact more strongly with Ce:YAG through its carbonyl oxygen, as previously observed. The storage modulus, loss modulus and glass transition temperature of PMMA increased with the addition of, and increase in, Ce:YAG content as a result of the increased stiffness of the composites and immobilization of the polymer chains. However, the extent of increase in the storage and loss modulus of the PC/Ce:YAG composites could not be related to the amount of filler in the respective samples. The glass transition was also not influenced by the presence of the filler, and the extent of damping changed inconsistently with the amount of filler in the samples, probably due to the weaker interaction between PC and Ce:YAG.

Acknowledgements The authors acknowledge the University of Palermo for supporting this research through the CORI2013 (Bando per la concessione di contributi per l'avvio e lo sviluppo di collaborazioni dell'Ateneo 2013- Azione D-prot. 32827 del 2/5/2013). The National Research Foundation in South Africa funded the bursary of the student who worked on this project.

References

1. Ramaanathan T, Stankovich S, Dikin DA, Liu H, Shen H, Nguyen ST, Brinson LC (2007) Graphitic nanofillers in PMMA nanocomposites—an investigation of particle size dispersion and their influence on nanocomposites properties. J Polym Sci, Part B: Polym Phys 45:2097–2112. doi:10.1002/polb.21187
2. Frogley MD, Ravich D, Wagner HD (2003) Mechanical properties of carbon nanoparticle-reinforced elastomers. Compos Sci Technol 63:1647–1654. doi:10.1016/S0266-3538(03)00066-6
3. Run MT, Wu SZ, Zhang DY, Wu G (2007) A polymer/mesoporous sieve composite: preparation, structure and properties. Mater Chem Phys 105:341–347. doi:10.1016/j.matchmphys.2007.04.070
4. Chow WS, Leu YY, Ishak ZM (2014) Poly(lactic acid) nanocomposites with improved impact and thermal properties. J Compos Mater 48:155–163. doi:10.1177/0021998312469891
5. Dacanin L, Lukic SR, Petrovic DM, Krsmanovic R, Cincovic MM, Dramicanin MD (2012) PMMA/Zn_2SiO_4:Eu^{3+}(Mn) composites: Preparation, optical, and thermal properties. J Mater Eng Perform 21:1509–1513. doi:10.1007/s11665-011-0049-3
6. Cincovic MM, Antic Z, Krsmanovic R, Mitric M, Dramicanin MD (2009) Thermal and luminescence properties of nano Gd_2O_3:Eu^{3+}/PMMA composite. J Optoelectron Adv Mater 1:54–58
7. Rai P, Song MK, Song HM, Kim JH, Kim YS, Lee IH, Yu YT (2012) Synthesis, growth mechanism and photoluminescence of monodispersed cubic shape Ce doped YAG nanophosphor. Ceram Int 38:235–242. doi:10.1016/j.ceramint.2011.06.057
8. Musbah SS, Radojevic V, Radovic I, Uskokovic PS, Stojanivic DB, Dramicanin M, Aleksic R (2012) J Min Metal 48:309–318. doi:10.2298/JMMB120508030M
9. Zarzeck-Napierala M, Haberko K (2007) Synthesis and characterization of yttrium aluminium garnet (YAG) powders. Process Appl Ceram 1:69–74
10. Marlot C, Barraud E, Gallet SL, Eichhorn M, Bernard F (2012) Synthesis of YAG nanopowder by co-precipitation method: influence of pH and study of the reaction mechanism. J Solid State Chem 191:114–120. doi:10.1016/j.jssc.2012.02.063
11. Wang J, Zheng S, Zeng R, Dou S, Sun X (2009) Microwave synthesis of homogenous YAG nanopowder leading to a transparent ceramic. J Am Ceram Soc 92:1217–1223. doi:10.1111/j.1551-2916.2009.03086.x

12. Saladino ML, Caponetti E, Martino DC, Enzo S, Ibba G (2008) Effect of the dopant selection (Er, Eu, Nd or Ce) and its quantity on the formation of yttrium aluminium garnet nanopowders. Opt Mater 31:261–267. doi:10.1016/j.optmat.2008.04.008
13. Katelnikovas A, Justel T, Uhlich D, Jorgensen JE, Sakirzanovas S, Kareiva A (2008) Characterization of cerium doped yttrium aluminium garnet nanopowders synthesized via sol-gel process. Chem Eng Commun 195:758–769. doi:10.1080/00986440701691194
14. Zarzecka M, Busko MM, Brzezinska-Miecznik J, Haberko K (2007) YAG powder synthesis by the modified citrate process. J Eur Ceram Soc 27:593–597. doi:10.1016/j.jeurceramsoc.2006.04.113
15. Yang H, Yuan L, Zhu G, Yu A, Xu H (2009) Luminescent properties of YAG:Ce^{3+} phosphor powder prepared by hydrothermal-homogeneous precipitation method. Mater Lett 63:2271–2273. doi:10.1016/j.matiet.2009.07.012
16. Kasuya R, Isobe T, Kuma H, Katano J (2005) Photoluminescence enhancement of PEG-modified YAG:Ce^{3+} nanocrystal phosphor prepared by glycothermal method. J Phys Chem B 109:22126–22130. doi:10.1021/jp052753j
17. Xia G, Zhou S, Zhang J, Xu J (2005) Structure and optical properties of YAG: Ce 3 + phosphors by sol-gel combustion method. J Cryst Growth 279:357–362. doi:10.1016/j.jcrysgro.2005.01.072
18. Kang YC, Lenggoro IW, Park SB, Okuyama K (2000) YAG: Ce phosphor particles prepared by ultrasonic spray pyrolysis. Mater Res Bull 35:78798
19. Yang Z, Li X, Yang Y, Li X (2007) The influence of different conditions on the luminescent properties of YAG: Ce phosphor formed by combustion. J Lumin 122–123:707–709. doi:10.1016/j.jlumin.2006.01.266
20. Caponetti E, Enzo S, Lasio B, Saladino ML (2007) Co-precipitation synthesis of neodymium-doped yttrium aluminium oxides nanopowders: quantitative phase investigation as a function of joint isothermal treatment conditions and neodymium content. Opt Mater 29:1240–1243
21. Saladino ML, Nasillo G, Chillura Martino D, Caponetti E (2010) Synthesis of Nd:YAG nanopowder using the citrate method with microwave irradiation. J Alloy Compd 491:737–741
22. Caponetti E, Chillura Martino D, Saladino ML, Leonelli C (2007) Preparation of Nd:YAG nanopowder in a confined environment. Langmuir 23:3947–3952
23. Mancic L, Marinkovic K, Marinkovic BA, Dramicanin M, Milosevic O (2010) YAG:Ce^{3+} nanostructure particles obtained via spray pyrolysis of polymeric precursor solution. J Eur Ceram Soc 30:577–582. doi:10.1016/j.jeurceramsoc.2009.05.037
24. M. Marinovic-Cincovic, Z. Antic, R. Krsmanovic, M. Mitric, M.D. Dramicanin. Thermal and luminescence properties of nano-Gd_2O_3:Eu^{3+}/PMMA composite. Journal of Optoelectronics and Advanced Materials—Symposia 2009; 1:54–58
25. Antic Z, Krsmanovic R, Marinovic-Cincovic M, Dramicanin MD (2010) Gd_2O_3:Eu^{3+}/PMMA composite: thermal and luminescence properties. Acta Phys Pol, A 117:831–836
26. Dacanin L, Lukic SR, Petrovic DM, Antic Z, Krsmanovic R, Marinovic-Cincovic M, Dramicanin MD (2012) PMMA/Zn_2SiO_4:Eu^{3+}(Mn^{2+}) composites: preparation, optical, and thermal properties. J Mater Eng Perform 21:1509–1513. doi:10.1007/s11665-011-0049-3
27. Saladino ML, Chillura Martino D, Floriano MA, Hreniak D, Marciniak L, Stręk W, Caponetti E (2014) Ce:$Y_3Al_5O_{12}$-polymethylmethacrylate composite for white-light-emitting diodes. J Phys Chem C 118:9107–9113
28. Zanotto A, Spinella A, Caponetti E, Luyt AS (2012) Macro-micro relationship in nanostructured functional composites. eXPRESS 6:410–416. doi:10.3144/expresspolymlett.2012.43
29. Hu YH, Chen CY, Wang CC (2004) Viscoelastic properties and thermal degradation kinetics of silica/PMMA nanocomposites. Polym Degrad Stab 84:545–553. doi:10.1016/j.polymdegradstab.2004.02.001
30. Motaung TE, Saladino ML, Luyt AS, Martino DFC (2012) The effect of silica nanoparticles on the morphology, mechanical properties and thermal degradation kinetics of polycarbonate. Compos Sci Technol 73:34–39. doi:10.1016/j.compscitech.2012.08.014
31. Dong Q, Gao C, Ding Y, Wang F, Wen B, Zhang S, Wang T, Yang M (2011) A polycarbonate/magnesium oxide nanocomposite with high flame retardancy. J Appl Polym Sci 123:1085–1093. doi:10.1002/app.34574
32. Wang H, Xu P, Zhong W, Shen L, Du Q (2005) Transparent poly(methyl methacrylate)/silica/zirconia nanocomposites with excellent thermal stabilities. Polym Degrad Stab 87:319–327. doi:10.1016/j.polymdegradstab.2004.08.015

33. Run MT, Wu SZ, Zhang DY, Wu G (2007) A polymer/mesoporous molecular sieve composite: preparation, structure and properties. Mater Chem Phys 105:341–347. doi:10.1016/j.matchemphys.2007.04.070
34. Patra N, Salerno M, Cozzoli PD, Barone AC, Ceseracciu L, Pignatelli F, Carzino R, Marini L, Athanassiou A (2012) Thermal and mechanical characterization of PMMA nanocomposites filled with TiO_2 nanorods. Compos B 43:3114–3119. doi:10.1016/j.compositesb.2012.04.028
35. Maiti S, Shrivastava NK, Suin S, Khatua BB (2013) A strategy for achieving low percolation and high electrical conductivity in melt-blended polycarbonate (PC)/multiwalled carbon nanotubes (MWCNT) nanocomposites: electrical and thermo-mechanical properties. eXPRESS. Polym Lett 7:505–518. doi:10.3144/expresspolymlett.2013.47
36. Hee HJ, Taek SY, Heon SK, Nylon KW, Byoung K, Lyong KS, Hong LC (2007) Morphology and dynamic mechanical properties of poly(acrylonitrile-butadiene-styrene)/polycarbonate/clay nanocomposites prepared by melt mixing. Instrum Sci Technol 14:519–532. doi:10.1163/156855407781291290
37. Motaung TE, Saladino ML, Luyt AS, Martino DC (2013) Influence of the modification, induced by zirconia nanoparticles, on the structure and properties of polycarbonate. Eur Polymer J 49:2022–2030. doi:10.1016/j.eurpolymj.2013.04.019
38. Musbah SS, Radojevic VJ, Borna NV, Stojanovic DB, Dramicanin MD, Marinkovic AD, Aleksic RR (2011) PMMA-$Y_2O_3(Eu^{3+})$ nanocomposites: Optical and mechanical properties. J Serb Chem Soc 76:1153–1161. doi:10.2298/JSC100330094M
39. Musbah SS, Radojevic VJ, Radovic I, Uskokovic PS, Stojanovic DB, Dramicanin M, Aleksic R (2012) Preparation, characterization and mechanical properties of rare-earth-based nanocomposites. J Min Metal 48:309–318. doi:10.2298/JMMB120508030M
40. Armetta F, Sibeko MA, Luyt AS, Martino DFC, Martino A, Saladino MA (2016) Influence of the Ce:YAG amount on structure and optical properties of Ce:YAG-PMMA composites for white LED. Z Phys Chem 230:1219–1231. doi:10.1515/zpch-2015-0703
41. Saladino ML, Armetta F, Sibeko MA, Luyt AS, Martino DFC, Caponetti E (2016) Preparation and characterization of Ce:YAG polycarbonate composites for white LED. J Alloys Compd 664:726731. doi:10.1016/j.jallcom.2016.01.009
42. Suin S, Shrivastava NK, Maiti S, Khatua BB (2013) Phosphonium modified organoclay as potential nanofiller for the development of exfoliated and optically transparent polycarbonate/clay nanocomposites: preparation and characterisation. Eur Polymer J 49:49–60. doi:10.1016/j.eurpolymj.2012.10.004
43. Motaung TE, Luyt AS, Saladino ML, Caponetti E (2013) Study of morphology, mechanical properties, and thermal degradation of polycarbonate-titania nanocomposites as function of titania crystalline phase and content. Polym Compos 34:164–174. doi:10.1002/pc.22389
44. Motaung TE, Saladino ML, Luyt AS, Martino DC (2013) Influence of the modification, induced by zirconia nanoparticles, on the structure and properties of polycarbonate. Eur Polymer J 49:2022–2030. doi:10.1016/j.eurpolymj.2013.04.019
45. Nielsen LE, Landel RF (1994) Mechanical properties of polymers and composites. Marcel Dekker Inc, New York
46. Hu Y-H, Chen C-Y, Wang C-C (2004) Viscoelastic properties and thermal degradation kinetics of silica/PMMA nanocomposites. Polym Degrad Stab 84:545–553. doi:10.1016/j.polymdegradstab.2004.02.001
47. Valandro SR, Lombardo PC, Poli AL, Horn MA Jr, Neumann MG, Cavalheiro CCS (2014) Thermal properties of poly(methyl methacrylate)/organomodified montmorillonite nanocomposites obtained by in situ photopolymerization. Materials Research 17:265–270. doi:10.1590/S1516-14392013005000173
48. Sibeko MA, Luyt AS, Saladino ML, Caponetti E (2016) Morphology, mechanical and thermal; properties of poly(methyl methacrylate)(PMMA) filled with mesoporous silica (MCM-41) prepared by melt mixing. J Mater Sci 51:3957–3970. doi:10.1007/s10853-015-9714-5
49. Assael MJ, Botsios S, Gialou K, Metaxa IN (2005) Thermal conductivity of polymethyl methacrylate (PMMA) and borosilicate crown glass BK7. Int J Thermophys 26:1595–1605. doi:10.1007/s10765-005-8106-
50. Bozi J, Czegeny Z, Meszaros E, Blazso M (2007) Thermal decomposition of flame retarded polycarbonate. J Anal Appl Pyrol 79:337–345. doi:10.1016/j.jaap.2007.01.001
51. Jang BN, Wilkie CA (2005) The thermal degradation of bisphenol A polycarbonate in air. Thermochim Acta 426:73–84. doi:10.1016/j.tca.2004.07.023

52. Singh B, Sharma N (2008) Mechanistic implications of plastic degradation. Polym Degrad Stab 93:561–584. doi:10.1016/j.polymdegradstab.2007.11.008
53. Maiti S, Shrivastava NK, Suin S, Khatua BB (2013) A strategy for achieving low percolation and high electrical conductivity in melt-blended polycarbonate (PC)/multiwall carbon nanotube (MWCNT) nanocomposites: electrical and thermo-mechanical properties. eXPRESS. Polymer Letters 7:505–518. doi:10.3144/expresspolymlett.2013.47
54. Gupta MC, Viswanath SG (1996) Role of metal oxides in the thermal degradation of bisphenol A polycarbonate. J Therm Anal 46:1671–1679. doi:10.1021/ie9700167
55. Vyazovkin S (1996) A unified approach to kinetic processing of nonisothermal data. Int J Chem Kinet 28:95–101. doi:10.1002/(SICI)1097-4601(1996)28:2<95:AID-KIN4>3.0.CO;2-G
56. Motaung TE, Luyt AS, Bondioli F, Messori M, Saladino ML, Spinella A, Nasillo G, Caponetti E (2012) PMMA-titania nanocomposites: properties and thermal degradation behaviour. Polym Degrad Stab 97:1325–1333. doi:10.1016/j.polymdegradstab.2012.05.022
57. Aigbodion VS, Hassan SB, Atuanya CU (2012) Kinetics of isothermal degradation studied by thermogravimetric data: Effect of orange peels ash on thermal properties of high density polyethylene. J Mater Environ Sci 3:1027–1036
58. Hu YH, Chen CY, Wang CC (2004) Viscoelastic properties and thermal degradation kinetics of silica/PMMA nanocomposites. Polym Degrad Stab 84:545–553. doi:10.1016/j.polymdegrastab.2004.02.001
59. Mintao R, Dayu Z, Sizhu W, Gang W (2007) Thermal decomposition of poly(ethylene terephthalate)/mesoporous molecular sieve composites. Front Chem Eng China 1:50–54. doi:10.1007/s11705-007-0010-z